

# Numerical prediction of tropical cyclone motion

MUKUT B. MATHUR

National Meteorological Center, Washington, DC 20233

**सार**— महीन जाली अर्द्ध लंबांजी पूर्वग समीकरण निदर्श (मॉडल) की सहायता से प्रसंजनों की गति को ज्ञात किया गया है। विभिन्न आकार और तीव्रता वाले सममित भ्रमिनों और एक रूप स्टीयरिंग धारा का प्रयोग करते हुए यह निदर्श 72 घण्टों में समाकलित किया गया है। प्रत्येक स्थिति में भ्रमिल प्रसंजन की तीव्रता को तीव्र करता पाया गया है और पवन क्षेत्र में बृहद असममित विकसित होते हैं। असममितताओं की संरचना को चर्चा की गई है। यह बताया गया है कि तूफान की गति इन असममितताओं की संरचना से सम्बन्धित है।

**ABSTRACT.** The motion of hurricanes is investigated with a fine-mesh quasi-Lagrangian primitive equation model. The model is integrated to 72 hours using symmetric vortices of different size and intensity, and a uniform steering current. The vortex is found to intensify to hurricane strength in each case, and large asymmetries in the wind field develop. The structure of the asymmetries is discussed. It is suggested that the motion of the storms is related to the structure of these asymmetries.

## 1. Introduction

A Quasi-Lagrangian Model (QLM) has recently been implemented at the National Meteorological Center for the operational prediction of hurricanes. A description of the QLM, and its performance during 1987 hurricane season over the Atlantic are presented by Mathur (1988).

In the present investigation, numerical experiments are carried out with the QLM to study the motion of hurricanes using idealized initial states. Results show that the motion is governed not only by the steering current and the variation in the coriolis parameter but also by the effects of physical forcing (section 3).

## 2. Description of the model

The QLM can be integrated over any geographical area, and with any suitable horizontal and vertical resolution. Any appropriate cartesian grid (Polar stereographic, Lambert conformal or Mercator) can be used. The primitive equations with  $\sigma = p/p_s$  as the vertical coordinate are used. Here  $p$  is pressure, and  $p_s$  is the surface pressure. The two horizontal components of the wind ( $u, v$ ), the potential temperature  $\theta$ , the mixing ratio  $q$ , and the surface pressure are predicted. The vertical motion and the rainfall are diagnosed.

The variables are not staggered in the horizontal.  $u, v, \theta, q$  and geopotential  $\psi$  are defined in each layer. The vertical velocity  $\sigma$  is defined at the layer interfaces. The boundary conditions are  $\sigma = 0$  at the top (zero pressure) and the bottom of the model atmosphere.

Many physical processes such as the convective and non-convective release of latent heat, a dry convective adjustment procedure, the surface frictional effects, and sea to air transfer of sensible and latent heat are incorporated.

## 3. Numerical study of motion of storms

The impact of dynamical and physical forces on the motion of storms is studied using a uniform steering current and vortices of different size and intensity. A ten-layer version of the model with a grid spacing of 40 km was used on either an "f-plane", or on a Lambert conformal map projection. The eleven interfaces were located at the levels  $\sigma = 1.0, 0.95, 0.9, 0.8, 0.6, 0.4, 0.325, 0.25, 0.175, 0.1, 0$ . The initial vortex was located at the centre of the horizontal domain which consisted of  $111 \times 81$  grid points.

### (a) Initial vortex

The initial conditions for an axisymmetric vortex are derived from a procedure similar to the one used by Anthes *et al.* (1971). The surface pressure was set by the relations:

$$p(r) = p_0 - a \cos\left(\frac{\pi r}{R}\right), \quad \text{for } r < R \quad (1)$$

and

$$p(r) = p_0 + a, \quad \text{for } r > R$$

The initial wind field was obtained from the gradient wind equation:

$$\frac{v^2}{R} + f_c v = \frac{R_g T}{p_s} \frac{\partial p_s}{\partial r} + \frac{\partial \phi}{\partial r} \quad (2)$$

where  $v$  is the tangential wind in cylindrical coordinates and  $R_g$  is the gas constant. The temperature  $T$  is assumed to be constant on  $\sigma$  surfaces and is taken from a mean tropical atmosphere. Initially,  $\partial \phi / \partial r = 0$  and  $\partial p_s / \partial r$  is obtained from Eqn. (1), and Eqn. (2) is solved for  $v$ . The relative humidity is specified at the centre

TABLE 1

The relative humidity, at the centre and at large distances (> 2000 km) from the centre, in the experiments using an idealized initial state

Layer	RH at centre	RH beyond 2000 km
1	.99	.75
2	.95	.70
3	.90	.60
4	.85	.55
5	.80	.50
6	.80	.40
7	.75	.35
8	.73	.30
9	.70	.30
10	.70	.25

and at a large distance (>2000 km) from the centre (Table 1). A linear relation is used to interpolate relative humidity at all grid points. The vortex circulation is projected on the model's cartesian grid. The values of the variables on the lateral boundary points were unchanged throughout the forecast.

#### (b) Motion

A series of model integrations to 72 hr were performed with a uniform steering current (-5 m/s) superimposed over symmetric vortices. Three vortices defined by Eqn. (1) were used: (i) a small weak vortex SW ( $a=2$ ;  $R=400$  km, maximum wind of 11 m/s), (ii) a small strong vortex SS ( $a=6$ ,  $R=400$  km, maximum wind of 23 m/s), (iii) a strong large vortex SL ( $a=6$ ,  $R=800$  km, maximum wind of 17 m/s).

When using the "*f*-plane" and excluding all physical process parameterizations except horizontal diffusion, the initial vortices were displaced westwards with nearly the speed of the steering current and with little change in their intensity. When using the "*f*-plane" but including all physical process parameterizations, the initial vortices intensified to hurricane strength and were displaced northwestwards in all cases. The northward displacement was greatest in the mean for the larger vortex, the small strong vortex was displaced more northward than the small weak vortex (see Table 2). The three dimensional structure of the vortex is changed with the intensification and this change impacts the motion of the storm.

The model was also integrated to 72 hr using a Lambert conformal projection (thus providing for the beta effect of variable coriolis parameter). The northward displacement in the mean was nearly twice as great in the variable *f* cases than in the constant "*f*-plane" experiments. By 72 hr, the larger vortex was located 250 km northwest of the small strong vortex and 400 km northwest of the small weak vortex.

TABLE 2

The northward (N) and westward (W) components of the motion of the vortices (units: m/s). A uniform steering current (-5 m/s) is used

Vortex	0-24 hr		24-48 hr		48-72 hr		0-72 hr	
	N	W	N	W	N	W	N	W
<i>f</i> -Plane								
Small weak	0.00	-5.55	0.92	-4.16	0.46	-4.62	0.46	-4.77
Small strong	1.38	-6.01	0.00	-4.16	0.92	-5.09	0.77	-5.09
Large strong	-0.46	-6.48	2.70	-3.24	2.31	-5.09	1.52	-4.93
<i>Lambert conformal projection (variable f)</i>								
Small weak	0.25	-5.58	1.90	-4.31	1.14	-5.47	1.10	-5.12
Small strong	0.75	-5.70	1.78	-5.74	1.90	-5.53	1.48	-5.65
Large strong	0.13	-7.03	3.36	-5.47	3.43	-4.49	2.42	-5.66

According to the numerical results from a non-divergent barotropic model discussed by Chan and Williams (1987), the small strong vortex should have a larger northward displacement (northern hemisphere) due to  $\beta$ -effect than the small weak vortex. The northward velocity of the small strong vortex, when averaged over the entire 00-72 hr period, is larger than of the small weak vortex in the variable *f* case (Table 2). This result suggests that the northward displacement of the vortices in our experiments is determined by the  $\beta$ -effect in a fashion similar to that predicted by the barotropic model used by Chan and Williams.

It should be noted, however, that the northward velocity of the three vortices is not uniform throughout the 72-hr period. The small strong vortex moves with a northward velocity smaller than that of the small weak vortex between 24 & 48 hr and with a greater velocity in the other two periods. Notice that during the 24-48 hr period when the small strong vortex has smaller northward velocity than the small weak vortex in the variable *f* case, the small strong vortex has negligible northward velocity and the small weak vortex has substantial northward velocity on the *f*-plane. Also, note that the small strong vortex has larger northward velocity on the *f*-plane than in the variable *f* case during 00-24 hr period. The deviation of the motion of the storm from the motion implied by the steering current is not due to the  $\beta$ -effect alone, the physical forcing also has a large impact on the motion.

The change in the three dimensional structure of the vortex including its size, intensity, and the asymmetric structure (which may be considered as a modification of the steering current, see below) with time is not the same in the three cases when the physical forcing is included; the rate of change is also not uniform in any of the cases during the entire integration period. The northwestward displacement of the vortex is, therefore, not uniform and is also different from one case to

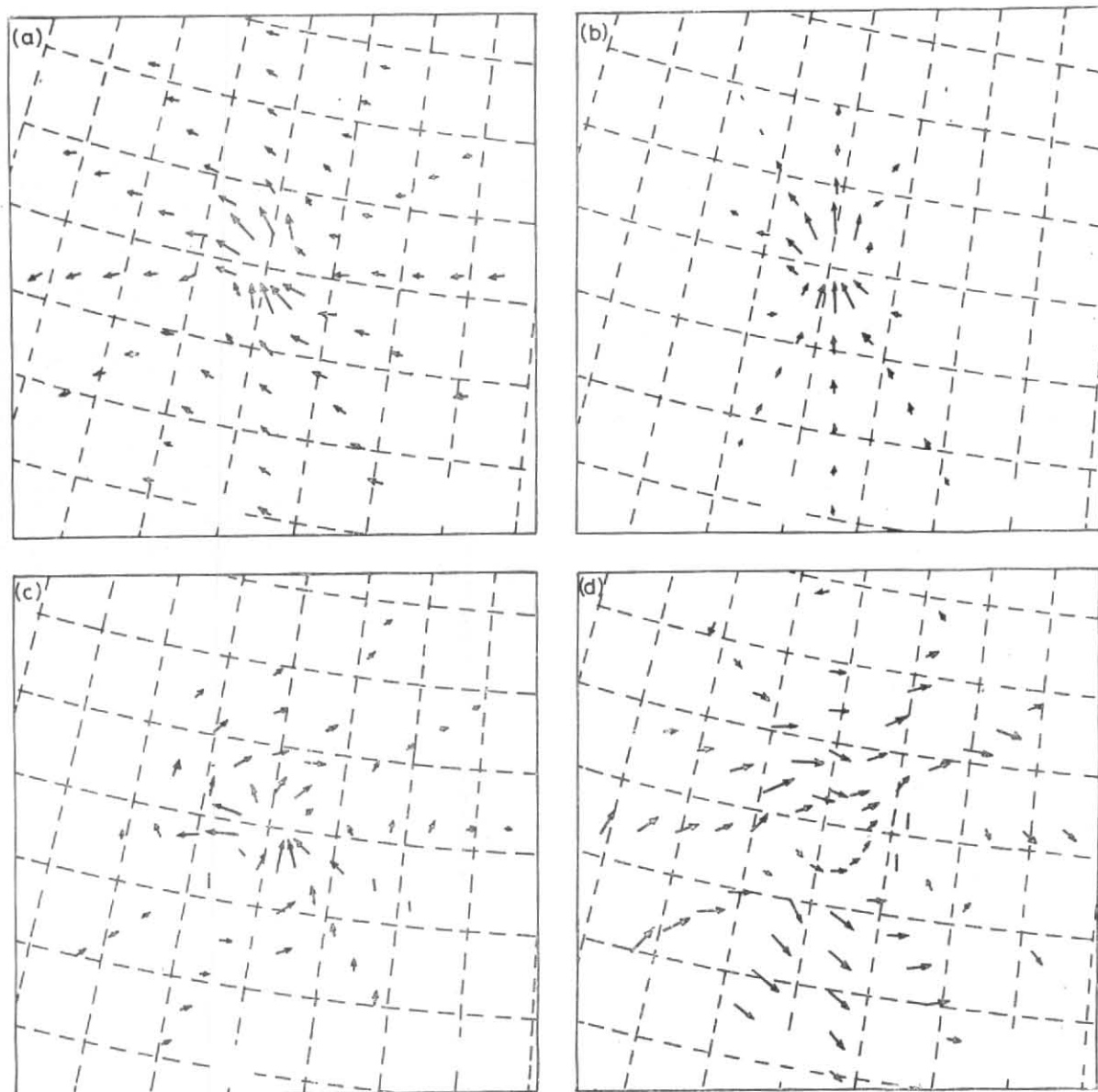


Fig. 1. The asymmetric structure of wind at 72 hr in a simulated hurricane. : (a) Total asymmetric winds at 850 mb. Developed asymmetric winds : (b) at 850 mb, (c) at 400 mb, and (d) at 250 mb. The winds are plotted on circles of radii  $1.6^\circ$  latitude. The latitude and longitude lines are drawn at an interval of  $2^\circ$ .

another. The results suggest that one cannot *a priori* deduce the displacement of a storm over sufficiently long period (several hours) from  $\beta$ -effect considerations alone.

#### (c) Asymmetric structure

The circulation in the small weak vortex when it intensified into a hurricane was very realistic. The maximum in the wind, pressure gradient and vertical motion were all located close (within 2-3 grid points) to the storm centre. The asymmetric part of the small weak vortex's circulation at 72 hr was calculated. The two horizontal components of the wind were first inter-

polated at 12 points equally spaced on a circle with centre at the storm's centre. The radial and the tangential components of the wind were then evaluated at each point. The symmetric part of the circulation was obtained by averaging the values of the two components. The asymmetric part of the flow was then calculated at each point by subtracting the average value of each component from its point value. The two components were then combined to give the vector winds for the asymmetric flow at each point. This procedure was repeated for circles of different radii and the results for 850 mb are presented in Fig. 1(a).

Recall that at the initial time, the asymmetric part of the wind is a specified easterly wind of 5 m/s. This asymmetric flow remains nearly unchanged in the regions far removed from the centre (radii greater than 400 km) in the lower troposphere. On the other hand, the asymmetric flow is quite different from the initial steering flow in the inner region ( $< 200$  km), where a strong southeasterly component has developed by 72 hr. This southeasterly flow is confined below 300 mb and is strongest at 850 mb. The displacement of the vortex to the right of the basic easterly steering current is related to the development of this southeasterly flow. The experimental results suggest that improved track forecasts may result with a more accurate specification (and prediction) of inner structure of storms.

The change in asymmetric wind that occurs with the intensification of the storm is obtained by subtracting the initial steering flow ( $-5$  m/s) from the (total) asymmetric flow. This change is referred to as the developed asymmetric wind flow, and is shown for 850, 400 and 250 mb in Figs. 1(b & c). The most noteworthy feature in the lower troposphere (Fig. 1b) is the zone of strong southerly winds (maximum 14 m/s) located within 100-200 km of the centre. A weak anticyclonic (cyclonic) circulation lies at a distance of 300-500 km to the east (west) of the centre. Qualitatively, this structure of developed asymmetric winds in the lower troposphere in the QLM is similar to the asymmetric flow that develops in other vortex models (e.g., Fiorino 1987) due to the  $\beta$ -effect. Fiorino imposed an isolated storm vortex as an initial condition in a non-divergent barotropic  $\beta$ -plane model. Both size and intensity of the vortex were varied in his experiments. All vortices were found to move northwestward. The asymmetric flow that developed during a forecast was also examined. Two gyres developed, one an anticyclonic circulation to the right, and the other a cyclonic circulation to the left of the track. A southerly flow with maximum wind of a few m/s (called the ventilation flow by Fiorino) developed over the storm vortex between the two gyres. This ventilation flow is found to be much stronger in the present experiment than in Fiorino's simple barotropic model. Many dynamical and physical effects (e.g., vertical advection, steering current, latent heating) that are included in our model, are not accounted for in Fiorino's model.

The structure of the developed asymmetric winds in the upper tropospheric outflow layer (Fig. 1d) is substantially different from its structure in the lower troposphere. The winds are mostly from the west (maximum

7.1 m/s). A ridge is located to the east and another ridge to the southwest of the centre. A cyclonic circulation lies to the north of the centre. The transition from the lower tropospheric flow to the upper tropospheric flow takes place near 400 mb (Fig. 1c). Except in a region close to the centre, the winds have a westerly component similar to but weaker than the winds in the upper troposphere.

#### (d) Discussion

The variables on the boundary were kept fixed throughout the integration in the above experiments. The developed asymmetric flow was very small beyond 600 km from the centre. It may, therefore, be argued that the developed asymmetric flow in the simulated storm represents the asymmetric flow which arises due to dynamic and physical forcing within the region of a storm. Our results show that this asymmetric flow has complex vertical and horizontal structure, and as noted above, the motion of the storm is related to this asymmetric wind flow.

#### 4. Remarks

Because of lack of data, the circulation of a storm is not well represented in the operational analysis. An idealized vortex is, therefore, superimposed on the analysis to simulate the observed storm. Numerical results that are presented above show that the motion of a tropical storm depends on its initial size and intensity. The size and intensity of the observed storm are, therefore, used to specify the idealized vortex in the operational QLM. An example of improvement in the track and intensity forecast with the use of the idealized vortex is presented by Mathur (1988).

#### References

- Anthes, R.A., Rosenthal, S.L. and Trout, J.W., 1971, Preliminary results from an asymmetric model of the tropical cyclone, *Mon. Weath. Rev.*, **99**, 744-758.
- Chan, J. C. L. and Williams, R. T., 1987, Analytical and numerical studies of the Beta-effect in tropical cyclone motion—Part I: Zero mean flow, *J. Atmos. Sci.*, **44**, 1257-1265.
- Fiorino, M., 1987, The role of vortex structure in tropical cyclone motion. Ph. D. dissertation, Naval Postgraduate School, Monterey, California.
- Mathur, M. B., 1988, The NMC Quasi-Lagrangian Hurricane Model, *Technical Procedure Bulletin*, **377**, National Weather Service, Silver Spring, Maryland.